JACS
JOURNAL OF THE AMERICAN CHEMICAL SOCIETY
Article
pubs.acs.org/JACS

Correlation between the Selectivity and the Structure of an Asymmetric Catalyst Built on a Chirally Amplified Supramolecular Helical Scaffold

Alaric Desmarchelier,[†] Xavier Caumes,[†] Matthieu Raynal,[*,†] Anton Vidal-Ferran,[‡,§] Piet W. N. M. van Leeuwen,[∥] and Laurent Bouteiller[†]

[†]Sorbonne Universités, UPMC Univ Paris 06, CNRS, Institut Parisien de Chimie Moléculaire, Equipe Chimie des Polymères, 4 Place Jussieu, F-75005 Paris, France

[‡]Institute of Chemical Research of Catalonia (ICIQ), Avgda. Països Catalans 16, 43007 Tarragona, Spain

[§]Catalan Institution for Research and Advanced Studies (ICREA), Passeig Lluís Companys 23, 08010 Barcelona, Spain

[∥]LPCNO, INSA, 135 Avenue de Rangueil, F-31077 Toulouse, France

Supporting Information

ABSTRACT: For the first time, supramolecular helical rods composed of an achiral metal complex and a complementary enantiopure monomer provided a good level of enantioinduction in asymmetric catalysis. Mixtures containing an achiral ligand monomer (**BTA**^{PPh2}, 2 mol %) and an enantiopure ligand-free comonomer (ester BTA, 2.5 mol %), both possessing a complementary benzene-1,3,5-tricarboxamide (BTA) central unit, were investigated in combination with $[Rh(cod)_2]BAr_F$ (1 mol %) in the asymmetric hydrogenation of dimethyl itaconate. Notably, efficient chirality transfer occurs within the hydrogen-bonded coassemblies formed by **BTA Ile** and the intrinsically achiral catalytic rhodium catalyst, providing the hydrogenation product with up to 85% ee. The effect of the relative content of **BTA Ile** as compared to the ligand was investigated. The amount of chiral comonomer can be decreased down to one-fourth of that of the ligand without deteriorating the enantioselectivity of the reaction, while the enantioselectivity decreases for mixtures containing high amounts of **BTA Ile**. The nonlinear relationship between the amount of chiral comonomer and the enantioselectivity indicates that chirality amplification effects are at work in this catalytic system. Also, right-handed helical rods are formed upon co-assembly of the achiral rhodium complex of **BTA**^{PPh2} and the enantiopure comonomer **BTA Ile** as confirmed by various spectroscopic and scattering techniques. Remarkably, the major enantiomer and the selectivity of the catalytic reaction are related to the handedness and the net helicity of the coassemblies, respectively. Further development of this class of catalysts built on chirally amplified helical scaffolds should contribute to the design of asymmetric catalysts operating with low amounts of chiral entities.

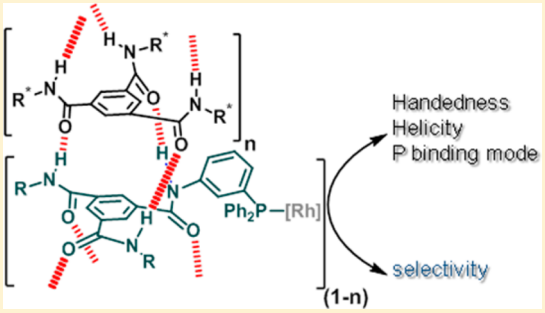

INTRODUCTION

Chirality amplification, the phenomenon by which a small asymmetric bias is translated into a large chiral preference, is a central topic of investigation mainly aimed at elucidating the origin of homochirality.[1] It also opens new avenues in the preparation of enantio-enriched molecules[2] and materials with promising perspectives of applications including the development of sensors,[3] stimuli-responsive gels,[4] liquid crystal displays,[5] stationary phases,[6] and catalysts.[7]

Chirality amplification effects are particularly strong in dynamic molecular helices,[8] such as those formed by covalent[9] and supramolecular polymers,[10] and foldamers,[8b,11] because a minimal energetic bias at the monomeric level is cooperatively transferred along the polymeric main chain. In particular, when a few enantiopure monomers (called "the sergeants") impose their handedness to a large number of achiral ones (called "the soldiers"), the macromolecular helicity obeys the sergeants-and-soldiers principle. Following the pioneering results of Green and co-workers on poly(isocyanates),[9a,12] this phenomenon has been observed experimentally in a great number of examples, which in turn have been consistently modeled at the theoretical level.[13] Such an approach is particularly appealing for the construction of asymmetric catalysts because it might enable a good control of the asymmetric environment around the metal center with a limited amount of chiral inducers.

Surprisingly, only very recently was chirality amplification in helical polymers applied for the first time in the construction of efficient asymmetric catalysts.[14] Suginome and co-workers[7a,c] demonstrated that covalent poly(quinoxaline-2,3-diyl)s terpolymers containing achiral phosphine monomers (0.4%), achiral phosphine-free monomers (82%),[15] and only 18% of

Received: February 4, 2016
Published: March 21, 2016

ACS Publications © 2016 American Chemical Society

DOI: 10.1021/jacs.6b01306
J. Am. Chem. Soc. 2016, 138, 4908–4916

Scheme 1. Possible Strategies [I]−[III] for the Construction of Supramolecular Helices Supporting Catalytic Metal Centers[a]

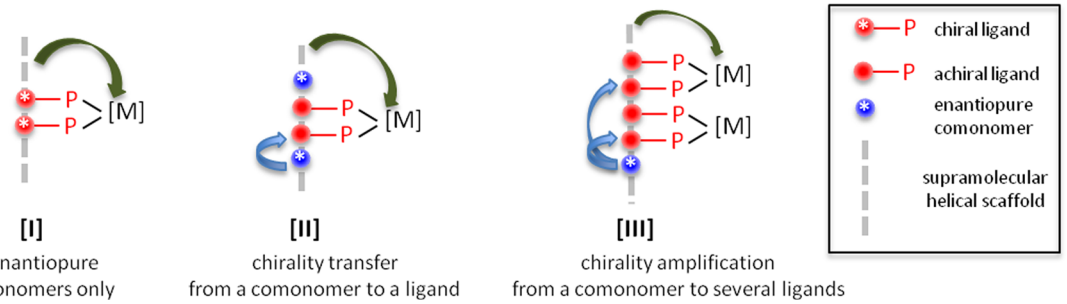

[a]The arrows illustrate the chirality transfers.

Chart 1. Structures of the BTA Ligands and Comonomers Used in the Asymmetric Hydrogenation Reaction

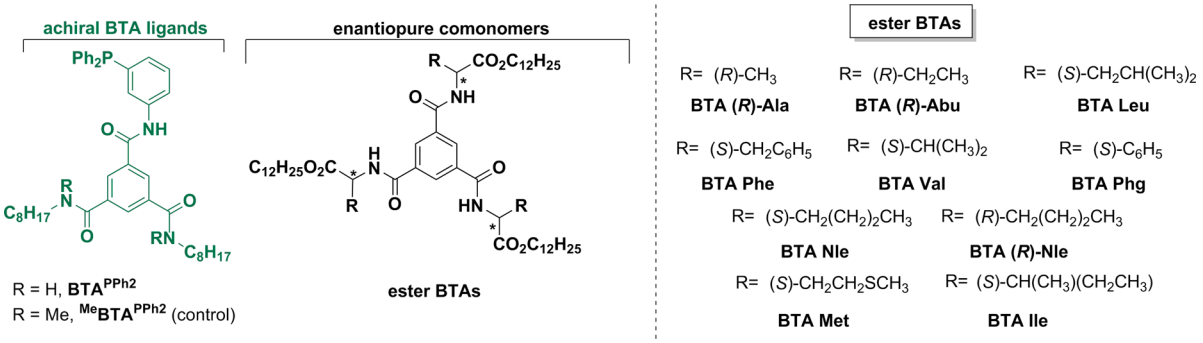

enantiopure monomeric units formed purely one-handed helical structures that promoted palladium-catalyzed asymmetric hydrosilylation and Suzuki−Miyaura cross-coupling reactions with remarkably high enantioselectivity.[16]

Helical supramolecular polymers also showed interesting features for catalysts development: (i) they are stimuli-responsive,[17] (ii) their supramolecular structure may enhance the activity and selectivity of catalytic centers arranged on their scaffold,[18] and (iii) their composition can be tuned by simply mixing different types of complementary monomers.[17b,19] Despite these promising achievements, little is known about how the chirality of a supramolecular polymer can be transferred to intrinsically achiral metal centers located at its periphery,[20] which can in turn be used as catalytic metals for asymmetric reactions.[19,21] One can envisage three strategies for the construction of chiral supramolecular helices supporting catalytic metal centers: the use of enantiopure monomers only ([I], Scheme 1), the use of a mixture of an achiral ligand monomer with a enantiopure ligand-free monomer in a nearly stoichiometric ratio ([II], chirality transfer), and the use of an enantiopure monomer as the minor component ([III], chirality amplification). While strategy [I] has already been successfully described,[19,21] strategies [II] and [III] remain to be implemented in an efficient way. The challenge in these cases is to obtain a good level of enantioinduction because any achiral metal catalysts that will not be located in a chiral environment will significantly decrease the selectivity of the reaction.[22] However, supramolecular copolymers used as efficient scaffolds for asymmetric catalysis should possess unique features: (i) they can be prepared by simply mixing the different monomers alleviating the synthetic efforts that are required for the preparation of covalent copolymers and (ii) chirality amplification effects that operate in these polymers can be used to decrease the amount of chiral inducers required to promote asymmetric catalysis.

Here, we demonstrate that supramolecular helical rods formed between an achiral rhodium complex of a benzene-1,3,5-tricarboxamide (BTA) ligand[23] and an enantiopure BTA comonomer can indeed be used as efficient scaffolds for the asymmetric hydrogenation of dimethyl itaconate (up to 85% ee). Chirality amplification effects are at work in this catalytic system, which allows decreasing the amount of chiral comonomer to one-fourth of that of the ligand monomer without deteriorating the enantioselectivity of the catalytic reaction. Moreover, we show that the selectivity of the catalytic reaction is related to the structure of the coassemblies, and notably to their helicity (as measured by CD spectroscopy), which may facilitate further development of this unique class of catalysts.

RESULTS AND DISCUSSION

The magnitude of chirality transfer and chirality amplification effects displayed by supramolecular assemblies between achiral and enantiopure monomers depends, among other factors, on the nature of the monomers.[10] Ester BTAs (Chart 1) were chosen as chiral comonomers because they are derived from an important accessible chiral pool and can be prepared straightforwardly in two synthetic steps (see the Supporting Information).[24] When studied individually, ester BTAs exhibit unusual self-association properties in cyclohexane as compared to classically investigated alkyl BTAs[23] because the nature of the substituent at the stereogenic carbon and the concentration determine the nature of the dominant species in solution, that is, stacks or dimers. Moreover, preliminary results indicated that coassemblies formed between an achiral alkyl BTA and an ester BTA, used as the enantiopure comonomer, display strong chirality amplification effects.[24c]

DOI: 10.1021/jacs.6b01306
J. Am. Chem. Soc. 2016, 138, 4908−4916

Catalytic Experiments. Mixtures composed of an achiral BTA ligand (**BTA^{PPh2}**, 2 mol %), the metal precursor ([Rh(cod)$_2$]BAr$_F$, 1 mol %), and an enantiopure comonomer (ester BTA) were tested in the rhodium-catalyzed hydrogenation of dimethyl itaconate. Catalytic components were mixed in CH_2Cl_2 to ensure the formation of the Rh complex between **BTA^{PPh2}** and [Rh(cod)$_2$]BAr$_F$, and then CH_2Cl_2 was removed under vacuum and replaced by the solvent selected for catalysis. In the following, the molar ratio between the ester BTA and **BTA^{PPh2}** initially present in the catalytic mixtures will be designated as $R^0_{esterBTA}$.

Chirality Transfer. The ease of preparation of the catalytic mixtures allowed us to test 10 ester BTAs ($R^0_{esterBTA}$ = 1.25) as potential enantiopure comonomers for the catalytic reaction (Table 1). In hexane/CH_2Cl_2 (10:1), the hydrogenation product of dimethyl itaconate was obtained with significant ee (enantiomeric excess) for all ester BTAs.

Table 1. Asymmetric Hydrogenation of Dimethyl Itaconate with Mixtures of BTA Ligand, [Rh(cod)$_2$]BAr$_F$, and Ester BTA: Screening of Various Comonomers[a]

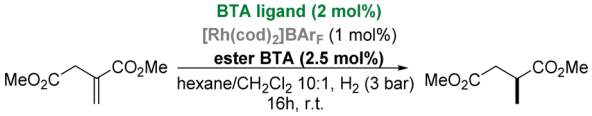

entry	BTA ligand	comonomer	ee (%)
1	**BTA^{PPh2}**	**BTA Phe**	40 (*S*)
2	**BTA^{PPh2}**	**BTA (*R*)-Ala**	−46 (*R*)
3	**BTA^{PPh2}**	**BTA Met**	53 (*S*)
4	**BTA^{PPh2}**	**BTA Leu**	54 (*S*)
5	**BTA^{PPh2}**	**BTA Phg**	62 (*S*)
6	**BTA^{PPh2}**	**BTA (*R*)-Abu**	−66 (*R*)
7	**BTA^{PPh2}**	**BTA (*R*)-Nle**	−72 (*R*)
8	**BTA^{PPh2}**	**BTA Nle**	74 (*S*)
9	**BTA^{PPh2}**	**BTA Val**	85 (*S*)
10	**BTA^{PPh2}**	**BTA Ile**	85 ± 7 (*S*)[b]
11	**^{Me}BTA^{PPh2}**	**BTA Ile**	0
12		**BTA Ile**	0
13[c]	**BTA^{PPh2}**	**BTA Ile**	nd

[a] $R^0_{esterBTA}$ = 1.25, n^0**BTA^{PPh2}** = 4.0 μmol, [dimethyl itaconate] = 0.4 M. Full conversion except for entry 13. Each experiment was performed in triplicate (except for control experiments 11−13), and the indicated ee corresponds to the average value (standard deviation ≤5%). Positive value of the ee corresponds to the (*S*) enantiomer.[25] See Chart 1 for the structures of the BTAs. See the Supporting Information for more details on the preparation of the catalytic mixtures. [b]Based on repeatability tests (16 runs, Table S1). [c]The catalytic mixture is filtered and catalysis is performed with the supernatant; no hydrogenation product was obtained. nd = not determined.

The selectivity of the catalytic reaction strongly depends on the nature of ester BTA (40% ee < selectivity <85% ee), thus showing the importance of having a library of enantiopure comonomers at one's disposition for catalytic screening. **BTA Ile** (entry 10) and **BTA Val** (entry 9) provided the (*S*) enantiomer of the hydrogenation product with the best selectivity (85% ee), a selectivity similar to that obtained with chiral monomers ([I], Scheme 1).[19] By inverting the chirality of the comonomer, we were able to access both enantiomers of the hydrogenation product with the same BTA ligand. For example, comonomers **BTA Nle** and **BTA (*R*)-Nle** furnish opposite enantiomers with similar ee values (74% and 72% ee, respectively, entries 7 and 8). Control experiments (entries 11, 12) confirmed that the selectivity of the reaction stems from the formation of hydrogen-bonded coassemblies between the rhodium complex of **BTA^{PPh2}** and ester BTAs. Indeed, **^{Me}BTA^{PPh2}**, a BTA ligand in which the amide groups have been *N*-methylated (Chart 1),[19] shows no selectivity in the presence of **BTA Ile** (entry 11). **BTA Ile** alone provided no ee either, demonstrating that ester BTAs do not influence the stereochemical outcome of the catalytic reaction by fortuitous coordination to the Rh center (entry 12).

We performed additional catalytic experiments with mixtures composed of **BTA^{PPh2}** and **BTA Ile** (R^0_{BTAIle} = 1.25, Tables 2 and S2). For catalytic experiments conducted in a mixture of hexane/CH_2Cl_2 10:1, the results were repeatable with a mean value of 85 ± 7% ee based on 16 runs (entry 1, Tables 2 and S1). The amount of CH_2Cl_2 in this solvent mixture can be increased to 20% without altering the selectivity (entry 2). However, the selectivity significantly decreases in a more polar hexane/CH_2Cl_2 2:1 mixture and in toluene, and no selectivity is obtained in CH_2Cl_2 (entries 3−5). This is related to the disruption of the hydrogen-bonded assemblies in these solvents.[19] In pure hexane, the selectivity appears to vary significantly from one run to another presumably because catalyst aggregates of variable size form under these conditions (Table S2 and vide infra). Changing the nature of the alkane solvent does not significantly influence the selectivity outcome of the reaction (Table S2).[26] While a lower concentration in substrate does not change the selectivity (entry 6), the ee significantly drops at higher substrate concentration perhaps as a result of competitive interactions between the substrate and the hydrogen-bonded assemblies (entry 7). Finally, lowering the temperature (−20 °C) leads to a decrease in the selectivity (entry 8 and Table S2).

Table 2. Screening of the Catalytic Conditions with BTA Ile as the Comonomer (R^0_{BTAIle} = 1.25)[a]

entry	solvent	[dimethyl itaconate] (M)	ee (%)
1	hexane/CH_2Cl_2 10:1	0.4	85 ± 7 (*S*)[b]
2	hexane/CH_2Cl_2 5:1	0.4	85 (*S*)
3	hexane/CH_2Cl_2 2:1	0.4	52 (*S*)
4	toluene	0.4	51 (*S*)
5	CH_2Cl_2	0.4	0
6	hexane/CH_2Cl_2 10:1	0.2	85 (*S*)
7	hexane/CH_2Cl_2 10:1	0.8	55 (*S*)
8	hexane/CH_2Cl_2 10:1	0.4	74 (*S*)[c]

[a]BTA^{PPh2} (2 mol %), [Rh(cod)$_2$]BAr$_F$ (1 mol %), BTA Ile (2.5 mol %), room temperature unless otherwise stated. Full conversion. Each experiment was performed in duplicate, and the indicated ee corresponds to the average value (standard deviation ≤5%). See Table S2 for additional screening experiments. [b]Based on repeatability tests (16 runs, Table S1). [c]Catalytic experiment performed at −20 °C.

These screening experiments reveal that both the nature of the enantiopure comonomer and the experimental conditions are crucial factors to obtain optimal selectivity for these catalytic systems. Taken all together, these results indicate that the supramolecular chirality displayed by coassemblies formed between an achiral ligand monomer and an enantiopure comonomer ($R^0_{esterBTA}$ = 1.25) can be efficiently transferred to the peripheral rhodium centers, which in turn promote the

DOI: 10.1021/jacs.6b01306
J. Am. Chem. Soc. 2016, 138, 4908−4916

hydrogenation reaction with very good enantioselectivity ([II], Scheme 1).

Chirality Amplification. Encouraged by our initial screening performed with $R^0_{esterBTA}$ = 1.25, we probed the influence of the amount of enantiopure comonomer on the selectivity of the catalytic reaction. **BTA Ile**, one of the two most efficient ester BTAs, was selected and was mixed in variable amounts (0.1−8 mol %) to fixed quantities of **BTA**^{PPh2} (2 mol %, n^0**BTA**^{PPh2} = 4.0 μmol) and [Rh(cod)$_2$]BAr$_F$ (1 mol %).[27] The enantioselectivity of the hydrogenation reaction exhibits a strong dependence on R^0_{BTAIle} (Figure 1, R^0_{BTAIle} = n^0**BTAIle**/n^0**BTA**^{PPh2}). In fact, 48% ee is observed for the mixture containing the lowest amount of **BTA Ile** (R^0_{BTAIle} = 0.05, that is, 0.1 mol % loading in **BTA Ile**), and then the ee increases up to a plateau at 78−85% ee for 0.25 ≤ R^0_{BTAIle} ≤ 1.25 and then decreases for R^0_{BTAIle} > 1.25. The nonlinear increase of the selectivity of the catalytic reaction (see inset in Figure 1) as a function of R^0_{BTAIle} clearly reveals that chirality amplification effects are at work in this catalytic system ([III], Scheme 1). As a result of these chirality amplification effects, the amount of enantiopure comonomer can be decreased down to one-fourth of that of the ligand (i.e. one chiral molecule for two metal atoms) without deteriorating the enantioselectivity of the catalytic reaction. Further characterization is required to relate the chirality amplification effects displayed by this catalyst to the net helicity of the coassemblies, that is, to the bias between left- and right-handed helical fragments. Also, these effects alone cannot explain the entire selectivity outcome of the catalytic reaction as the enantioselectivity decreases at higher R^0_{BTAIle} values (R^0_{BTAIle} ≥ 1.5). This suggests that the structure of the catalyst evolves as a function of the composition of the coassemblies (vide infra).[28]

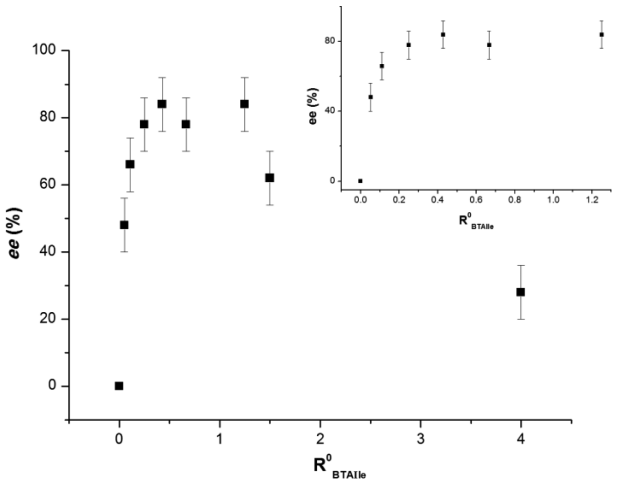

Figure 1. Enantioselectivity of the hydrogenation reaction as a function of R^0_{BTAIle}. R^0_{BTAIle} = n^0**BTA Ile**/n^0**BTA**^{PPh2}. Inset: Zoom of the region for values of R^0_{BTAIle} < 1.5.

Nature of the Catalytically Active Coassemblies. To rationalize the catalytic results, it is important to gain information into the assembly process and on the solubility properties of the resulting coassemblies. First, the catalytic mixture (**BTA**^{PPh2}+**BTA Ile**+[Rh(cod)$_2$]BAr$_F$) is prepared in CH_2Cl_2, a solvent in which no selectivity is observed, suggesting that coassembly between **BTA**^{PPh2} coordinated to Rh and **BTA Ile** does not occur to a significant extent (Table 2). In fact, coassembly likely occurs upon evaporation of CH_2Cl_2, and the rhodium complex remains insoluble as we observed no significant dissolution of the resulting yellow solid upon addition of hexane/CH_2Cl_2 10:1, the solvent mixture used in the catalytic experiments. However, this second solvent does have an influence on the size of the solid aggregates as we observed well-dispersed aggregates in hexane/CH_2Cl_2 mixtures but not in pure hexane (Table S2). We also found that the supernatant obtained after filtration of this yellow solid is not catalytically active (Table 1, entry 13). If we consider that the solubility of the coassemblies does not evolve during the catalytic reaction, then this result suggests that the reaction is actually catalyzed by insoluble coassemblies formed between the rhodium complex of **BTA**^{PPh2} and **BTA Ile** after evaporation of CH_2Cl_2.

Characterization of the Assemblies. With the objective of correlating the selectivity of the catalytic reaction with the structure of the BTA assemblies, we precisely probed the homo- and coassembly properties of **BTA**^{PPh2} and **BTA Ile**, in solution and in the solid state, by means of Fourier transform-infrared (FT-IR) spectroscopy, UV absorption, circular dichroism (CD), and small-angle neutron scattering (SANS) analyses. These analyses were performed both in the presence and in the absence of Rh coordinated to **BTA**^{PPh2}.

Homoassemblies. When studied separately, **BTA**^{PPh2} and **BTA Ile** display different association properties in cyclohexane.[29] **BTA**^{PPh2} forms long and rigid stacks (Figure S1) as shown by (i) FT-IR bands at 3245 cm^{-1} (NH bonded to amide CO), 1634, and 1549 cm^{-1} (amide CO bonded to NH, amide I and II bands, respectively), and (ii) the q^{-1} dependence of the SANS intensity at low q values characteristic of isolated cylindrical rigid rods (r = 12.6 Å, L > 200 Å). In striking contrast, **BTA Ile** only forms dimers in which the amide NH's are linked to the ester carbonyl instead of the amide carbonyl. **BTA Ile** does not form stacks across the whole range of concentration investigated (0.05−50 mM). The dimers of **BTA Ile** possess the same spectroscopic and scattering signature as those previously characterized for **BTA Nle**[24c] (for a proposed molecular arrangement and analyses, see Figure S2). The assembly of **BTA Ile** into dimers in cyclohexane is in sharp contrast with its ability to form stacks in the solid state (Figure S3). The positive Cotton effect observed above 200 nm in CD analyses infers the preferential formation of right-handed helical stacks[30] of **BTA Ile** as was previously found in the X-ray structure of a related ester BTA.[31]

Importantly, the rhodium complex formed by reacting **BTA**^{PPh2} with [Rh(cod)$_2$]BAr$_F$, in a 2:1 ratio, is soluble in CH_2Cl_2 but not in cyclohexane. UV and FT-IR analyses of the thus obtained solid indicate that this rhodium complex assembles into stacks (Figure S4b,c). As expected, given that **BTA**^{PPh2} is achiral, these stacks show no helical preference (Figure S4a).

Composition and Structure of the Coassemblies. Upon mixing two complementary monomers, one can envisage (i) the formation of their homoassemblies exclusively (narcissistic self-sorting), (ii) the formation of coassemblies exclusively (social self-sorting), and (iii) an intermediate situation in which homo- and coassemblies are concomitantly present. Determining whether the coassembly process follows one of the above hypotheses (i−iii) is challenging particularly when the species have similar analytical signatures. In our case, stacks and dimers can be easily differentiated by means of spectroscopic and scattering analyses, which allow us to precisely determine the composition and structure of the coassemblies. Mixtures of

DOI: 10.1021/jacs.6b01306
J. Am. Chem. Soc. 2016, 138, 4908−4916

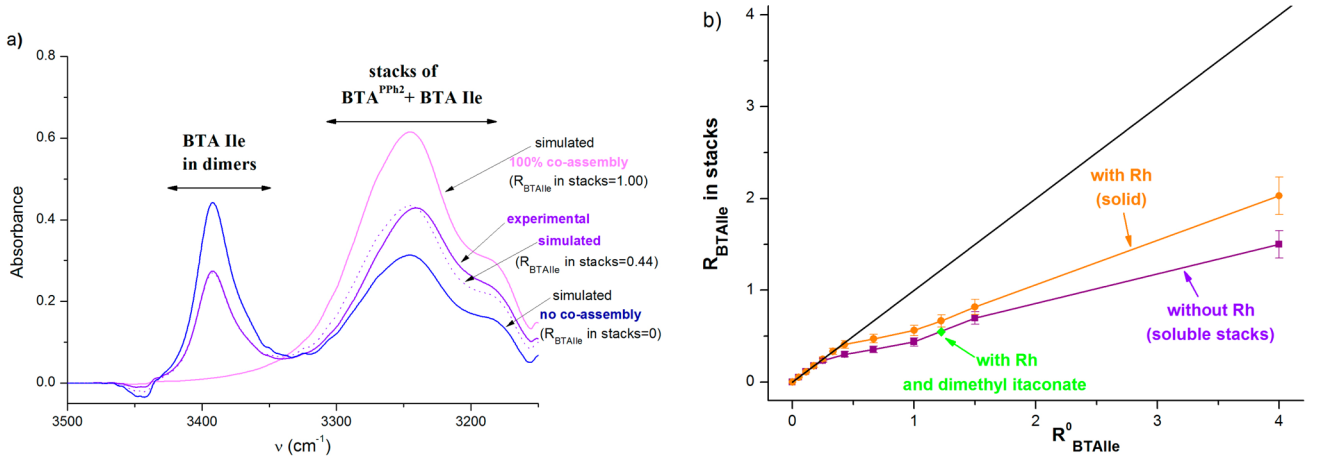

Figure 2. Quantification of the amount of **BTA Ile** present in the coassemblies. Left: FT-IR spectrum (zoom of the NH region) of the mixture of **BTA**^{PPh2} and **BTA Ile** (R^0_{BTAIle} = 1.00, [**BTA**^{PPh2}]^0 = 8.0 mM) in cyclohexane. Simulated spectra for the extreme cases for which all or no **BTA Ile** is present in the coassemblies. R_{BTAIle} in stacks (here 0.44) is deduced from the amount of **BTA Ile** in dimers. Right: R_{BTAIle} in stacks as a function of R^0_{BTAIle} (with or without Rh coordinated to **BTA**^{PPh2}). For the coassemblies in the presence of Rh, the amount of **BTA Ile** in the insoluble stacks is deduced from the amount of **BTA Ile** that remains as dimers in the cyclohexane phase. The black line ($y = x$) helps to visualize mixtures for which **BTA Ile** is fully incorporated into stacks. R_{BTAIle} in stacks = n**BTA Ile** in stacks/n^0**BTA**^{PPh2}.

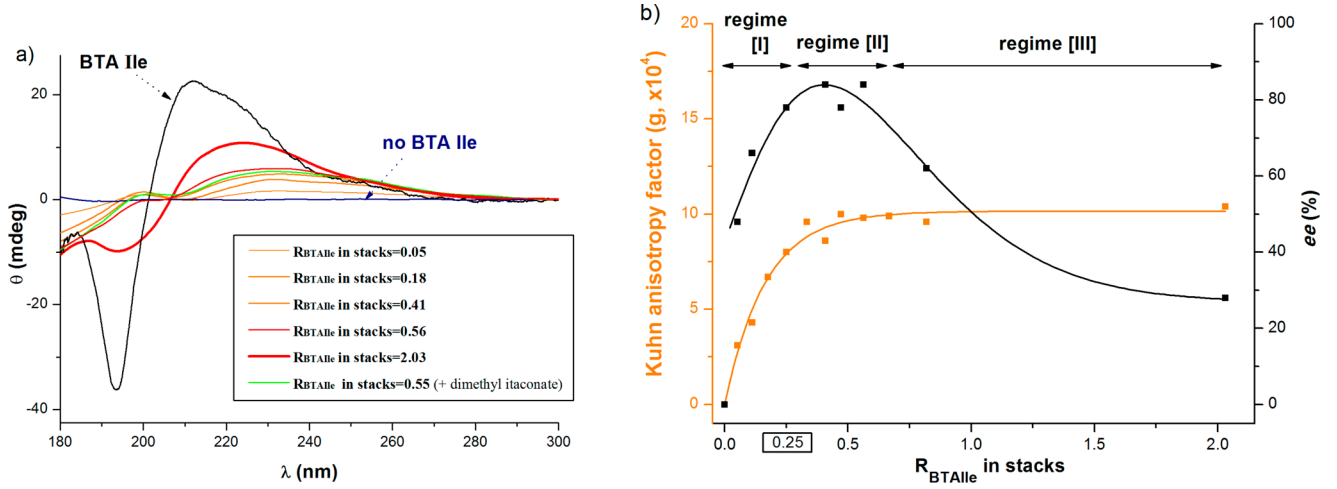

Figure 3. (a) CD spectra of the coassemblies formed between the rhodium complex of **BTA**^{PPh2} (8 μmol in **BTA**^{PPh2} for all mixtures) and **BTA Ile**. For the CD spectra of all of the mixtures, see Figure S9. (b) Plots of the anisotropy factor (g) of coassemblies and of the enantioselectivity of the hydrogenation reaction as a function of R_{BTAIle} in stacks. The lines are drawn to guide the eye. g values measured at λ = 249.0 nm.

BTA^{PPh2} and **BTA Ile**, with a fixed amount of **BTA**^{PPh2} and variable amounts of **BTA Ile** ($0.05 \leq R^0_{BTAIle} \leq 4.0$), proved to be fully soluble in cyclohexane. For mixtures with $R^0_{BTAIle} \leq 0.18$, FT-IR analyses show that all BTA monomers are in stacks inferring that all **BTA Ile** monomers are incorporated into the coassemblies (case ii above). In contrast, for other mixtures, FT-IR analyses indicate both the presence of stacks and dimers, suggesting that **BTA Ile** only partly coassembles with **BTA**^{PPh2} (case iii). In that case, the quantity of **BTA Ile** that is incorporated into the stacks is deduced from the amount of **BTA Ile** that remains as dimers as measured by FT-IR (Figures 2a and S5) and SANS analyses (Figure S6). Accordingly, coassemblies are observed for all mixtures (Table S3), and the ratio of **BTA Ile** that actually coassembles with **BTA**^{PPh2} is defined as R_{BTAIle} in stacks = n**BTA Ile** in stacks/n^0**BTA**^{PPh2}.

The same approach can be applied to mixtures of **BTA**^{PPh2}, **BTA Ile**, and [Rh(cod)$_2$]BAr$_F$ to determine the composition of the coassemblies between the rhodium complex of **BTA**^{PPh2} and **BTA Ile**. Here, all mixtures form heterogeneous suspensions in cyclohexane and characterization of the soluble part indicates that it only contains **BTA Ile** (in the form of dimers, Figure S8); that is, all Rh and all ligand is in the solid. For all mixtures, the amount of **BTA Ile** in the soluble phase is significantly lower than the quantity of **BTA Ile** initially introduced in the mixtures, which indicates (and allows us to quantify) the presence of **BTA Ile** in the solid (Table S4). It is important to note that the presence of **BTA Ile** in the solid demonstrates its coassembly with the Rh complex of **BTA**^{PPh2} because **BTA Ile** is fully soluble in cyclohexane. Thus, in contrast to coassemblies without Rh, the coassemblies between **BTA Ile** and the rhodium complex of **BTA**^{PPh2} are insoluble and can be isolated from nonincorporated dimers of **BTA Ile** by simple centrifugation.

R_{BTAIle} in stacks can be plotted as a function of R^0_{BTAIle} (Figure 2b). For both types of coassemblies (with and without Rh), the same trend is observed. **BTA Ile** is quantitatively incorporated into the coassemblies for mixtures with $R^0_{BTAIle} < 0.25$. For higher **BTA Ile** contents, the incorporation of **BTA**

DOI: 10.1021/jacs.6b01306
J. Am. Chem. Soc. 2016, 138, 4908−4916

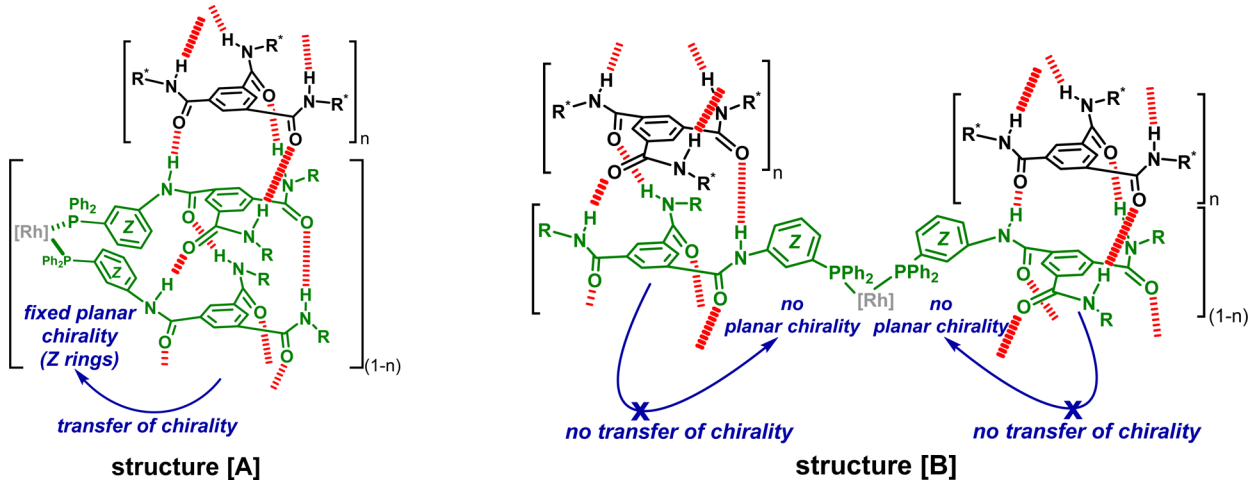

Figure 4. Proposed supramolecular structures [**A**] and [**B**] for the catalysts and postulated mechanism for the chirality transfer.

Ile in the coassemblies levels off (plateau value at R_{BTAIle} in stacks ≈ 0.3−0.5) and then increases again for $R^0_{BTAIle} \geq 1.0$. This nonuniform trend can be explained by potentially different thermodynamic stabilities displayed by the coassemblies depending on their content in **BTA Ile**. Interestingly, the ratios of **BTA Ile** present in both types of coassemblies (with or without Rh) are virtually the same. It suggests that the coordination of the $[Rh(cod)]^+$ fragment to **BTA**^{PPh2} does not significantly modify the composition of the coassemblies.

The structure of the coassemblies between **BTA Ile** and the Rh complex of **BTA**^{PPh2} was then probed in the solid state by UV and FT-IR analyses (Figure S9). Despite their different compositions (Figure 2a), similar spectra with bands that are characteristic of the stack form were observed for all mixtures. Accordingly, the different selectivities displayed by the coassemblies for the catalytic reaction cannot be related to a change in the association pattern of the central BTA units.

Chirality of the Coassemblies. The chirality of the coassemblies, with and without Rh, was then probed by CD spectroscopy. For mixtures of **BTA**^{PPh2} and **BTA Ile** (soluble coassemblies), CD spectra must be interpreted carefully because dimers of **BTA Ile** may contribute to the overall CD signals. Importantly, for mixtures with $R^0_{BTAIle} \leq 0.25$, a Cotton effect is observed, the shape of which is similar to that commonly found in CD spectra of BTA helical stacks exhibiting a preferred handedness in the solid state[32] and in solution[23,30] (Figure S7). A similar positive Cotton effect is observed in the CD spectra of the mixtures with Rh (insoluble coassemblies, Figures 3a and S9),[33] indicating that in both cases right-handed helical stacks are formed.[30] Clearly, **BTA Ile** imposes its preferred handedness (as observed for its helical stacks in the solid state, Figure S3) to the achiral ligand monomers.

Subsequently, the helicity of the coassemblies between the Rh complex of **BTA**^{PPh2} and **BTA Ile** was measured for all of the mixtures and expressed by the Kuhn anisotropy factor ($g = \Delta\varepsilon/\varepsilon$ at λ = 249.0 nm). As expected for helical assemblies displaying chirality amplification properties, the helicity does not increase linearly as a function of the amount of enantiopure monomer in the coassemblies (i.e., as a function of R_{BTAIle} in stacks, Figure 3b). Maximum g values are reached for R_{BTAIle} in stacks ≥0.25, which coincides with the minimum content of chiral comonomer (R^0_{BTAIle} = 0.25) required to obtain the highest enantioselectivity for the hydrogenation reaction.

Rationalization of the Selectivity Outcome. The selectivity observed in the catalytic hydrogenation of dimethyl itaconate (major enantiomer and enantioselectivity) can be related to the structure of the coassemblies. First, the handedness of the stacks dictates the nature of the major enantiomer. Indeed, the (*R*) hydrogenation product was obtained with our previously investigated chiral BTA ligand[19] that formed left-handed helical stacks, whereas the (*S*) hydrogenation product is furnished by the rhodium catalyst supported by the right-handed helical coassemblies of **BTA**^{PPh2} and **BTA Ile**. Second, the net helicity of the coassemblies explains the first two regimes of the selectivity outcome of the catalytic reaction: stacks containing less than one **BTA Ile** monomer for four **BTA**^{PPh2} monomers (regime [I], Figure 3b) do not (all) have the same handedness, so the catalytic selectivity is not optimal. For stacks containing between ca. one-fourth and one-half of **BTA Ile** relative to **BTA**^{PPh2} (regime [II]), all of the stacks have the same handedness (although the composition is evolving), so the catalytic selectivity is roughly constant. For regimes [I] and [II], there is a direct correlation between the net helicity of the coassemblies formed between the Rh complex of **BTA**^{PPh2} and **BTA Ile** and the selectivity outcome of the catalytic reaction. It is further corroborated by the fact that dimethyl itaconate, the substrate of the catalytic reaction, has no significant influence on the nature of the coassemblies (Figures 2b and 3a), at least at the concentration used in our optimized conditions (Table 2).

According to our experimental results, the decrease in selectivity observed for mixtures containing higher content of enantiopure comonomer cannot be explained by a different structure or a lower net helicity of the stacks. To explain this decrease in selectivity (regime [III], Figure 3b), we propose that the binding mode of the PPh_2 units to the Rh center evolves with the composition of the coassembly (Figure 4). In structure [**A**], two neighboring diphenylphosphino (PPh_2) units maintained by the right-handed helical stacks[30] are well positioned to chelate one Rh center.[34] We hypothesize that within this structure, chirality transfer occurs from the right-handed helices of the polymeric scaffold to the connecting rings (labeled as rings Z in structures [**A**] and [**B**]) facing one another with their *Si,Si* (or *Re,Re*) faces,[35] and from there to the peripheral PPh_2 units, which may adopt the well-known C_2 quadrant configuration (regimes [I] and [II]). In contrast, increasing the amount of enantiopure comonomers in the

DOI: 10.1021/jacs.6b01306
J. Am. Chem. Soc. 2016, 138, 4908−4916

stacks reduces the probability of having two consecutive BTA ligands, which prevents the coordination of Rh by two PPh_2 units belonging to the same stack. Accordingly, in the speculative structure [**B**], Rh is acting as a bridge between two right-handed helical stacks, and although these stacks exhibit the same handedness, they cannot efficiently transfer their helical chirality via a planar chiral rearrangement of the rings Z to the environment of the Rh catalytic center (regime [III]).

On the basis of structures [**A**] and [**B**], a consistent rationale of the selectivity outcome of the catalytic reaction is obtained. In this specific catalytic system, CD experiments may be used to predict (i) the major enantiomer produced by the catalytic reaction and (ii) the minimum amount of chiral comonomer required to get the optimal selectivity.

CONCLUSIONS

The above results clearly reveal the potential of supramolecular helical coassemblies as efficient scaffolds for asymmetric reactions. Achiral rhodium complexes of BTA ligands, when combined with suitable enantiopure complementary comonomers, are located within the chiral environment displayed by the coassemblies and promote the hydrogenation of dimethyl itaconate with good level of enantioinduction. The selectivity of the catalytic reaction is correlated to the handedness, the helicity, and the binding mode of the PPh_2 units to the catalytic rhodium center. The handedness and the helicity are dictated by the enantiopure comonomer, while the preferred binding mode of the phosphine ligands is related to their relative position in the helical stacks. Importantly, the helicity of coassemblies is not proportional to the amount of enantiopure comonomer. Benefiting from the chirality amplification properties displayed by the coassemblies, optimal selectivity for the catalytic system can be obtained with the amount of chiral comonomer being one-fourth of that of the achiral ligand. Performing an asymmetric reaction with little or no help of chiral entities raises many fundamental questions with potentially important applications.[2c] To date, only very rare but fascinating examples of asymmetric autocatalysts are able to promote asymmetric reactions by chirality amplification of a minute chiral imbalance.[2d,h,36] To the best of our knowledge, the present asymmetric metal catalyst also constitutes the first example in which a substoichiometric amount of a chiral inducer relative to the achiral ligand can be used without eroding the stereoselectivity of the catalytic reaction. Helped by our proposed rationale of the selectivity outcome of the catalytic reaction, we are currently selecting combinations of achiral and chiral monomers on the basis of their chiroptical properties with the aim of further reducing the amount of chiral inducer needed to get optimal selectivity.

EXPERIMENTAL SECTION

Materials Preparation. All amino acids were purchased from Sigma-Aldrich or Alfa Aesar (99% ee) and used as received. Benzene-1,3,5-tricarbonyl chloride was purchased from Alfa Aesar, and dimethyl itaconate, 1-dodecanol *p*-TsOH·H_2O, carbonyldiimidazole, and trimesic acid were acquired from Sigma-Aldrich, and were used directly. The synthesis and characterization of **BTA^{PPh2}**,[19] **^{Me}BTA^{PPh2}**,[19] $[Rh(cod)_2]BAr_F$,[37] **BTA Met**,[24c] **BTA Phe**,[24c] **BTA Nle**,[24c] and **BTA (*R*)-Nle**[24c] have been described previously. The experimental details for the synthesis and characterization of the ester BTAs are provided in the Supporting Information. Racemic ester BTAs, (*rac*)-BTAs, were prepared for the purpose of determining the optical purity of (*R*)-BTAs and BTAs (enantiomeric and diastereomeric excesses, see the Supporting Information for analytical details).

Catalytic Experiments. Preparation of the catalytic system: Mother solutions of each component were prepared separately in dry CH_2Cl_2 without any precaution to exclude air or moisture. This solvent readily dissolves each compound listed below. The following mother solutions are required: ester BTA, 50.0 mM; BTA ligand, 40.0 mM; $[Rh(cod)_2]BAr_F$, 20.0 mM; dimethyl itaconate, 1.0 M. For catalytic reactions performed with variable amounts of **BTA Ile**, a 10.0 mM mother solution of **BTA Ile** was used. The components are then mixed together in glass vials suitable for a 24-well pressurized reactor (CAT-24 reactor provided by HEL) equipped with small magnetic stirring bars, in the following order: ester BTA (desired volume), BTA ligand (100 μL, 4 μmol), $[Rh(cod)_2]BAr_F$ (100 μL, 2 μmol), and dimethyl itaconate (200 μL, 200 μmol). The vials are left open and stirred overnight in a well-ventilated fume-hood (900 $m^3\ h^{-1}$ flow) to evaporate the CH_2Cl_2. The next day, the vials are dried under a 10^{-3} mbar vacuum for 1 h to obtain a dry, gum-like solid (the dried reaction mixture). Catalysis: The aforementioned dried reaction system is taken up (desired volume) in the desired solvent, sonicated for a few seconds to obtain a bright yellow suspension, briefly heated to solvent reflux, and then transferred to the CAT-24 reactor, which is sealed and set on a magnetic stirrer at room temperature and at 1000 rpm for 1 h. The reactor is then purged three times with hydrogen gas (3−5 bar) before pressurizing it again at 3 bar of H_2. The hydrogenation is performed at room temperature, 1000 rpm stirring, over 16 h without compensating H_2 consumption. Determination of the conversion and the enantiomeric excess: The conversion was determined by ^{1}H NMR after evaporation of the catalytic solutions under vacuum. The ee was measured by chiral GC (Betadex 225, capillary 30.0 m × 250 μm × 0.25 μm, flow = 1.5 mL/min, P_{He} = 17.6 psi, isotherm at 70 °C (10 min) then 2 °C/min until 95 °C, tr(*R*) = 27.5 min, tr(*S*) = 27.8 min). For examples of GC spectra (one racemate and the result of the catalytic reaction performed with **BTA Ile** (R^0_{BTAIle} = 1.25), **BTA^{PPh2}**, and $[Rh(cod)_2]BAr_F$), see the Supporting Information. Assignment of enantiomers was made according to published data.[25] In Tables 1, 2, S1, and S2, enantiomeric excesses in favor of the (*R*) enantiomer are set as negative values (those of the (*S*) enantiomer are positive).

Preparation of BTA^{PPh2} and BTA Ile Mixtures (without Rh) for Spectroscopic Analyses. For FT-IR analyses: Solutions at different R^0_{BTAIle} values were made using mother solutions of **BTA^{PPh2}** (40.0 mM in CH_2Cl_2) and **BTA Ile** (40.0 mM in CH_2Cl_2). The components are then mixed together in glass vials equipped with small magnetic stirring bars, in the following order: **BTA Ile** (desired volume) and **BTA^{PPh2}** (200 μL, 8 μmole). The vials are left open and stirred overnight in a fume-hood. The resulting solids were put under vacuum (10^{-3} mbar) for 3 h before the addition of 1.0 mL of cyclohexane and sonicated for a few seconds to obtain a solution ([**BTA^{PPh2}**] = 8.0 mM and 0.42 < [**BTA Ile**] < 32.0 mM). The solutions were briefly heated to reflux and cooled to room temperature before analyses. For CD analyses: Solutions with a fixed concentration in **BTA^{PPh2}** (1.0 mM) and variable concentrations in **BTA Ile** (0.05−4.0 mM) were prepared in the same way as solutions for FT-IR analyses. For SANS analyses: Solutions with a fixed concentration in **BTA^{PPh2}** (3.5 g dm^{-3}, 5.1 mM) and variable concentrations in **BTA Ile** (2.2 and 24.5 mM) were prepared in C_6D_{12} in the same way as solutions for FT-IR and CD analyses.

Preparation of the Rh Complex of BTA^{PPh2} and BTA Ile Mixtures for Spectroscopic Analyses. Rh-containing mixtures were prepared similarly to those used in the catalytic experiments (vide supra). Solutions at different R^0_{BTAIle} values were made using mother solutions of $[Rh(cod)_2]BAr_F$ (40.0 mM in CH_2Cl_2), **BTA^{PPh2}** (40.0 mM in CH_2Cl_2), and **BTA Ile** (40.0 mM in CH_2Cl_2). The components were then mixed together in an Eppendorf tube in the following order: **BTA Ile** (desired volume), **BTA^{PPh2}** (200 μL, 8 μmol), and $[Rh(cod)_2]BAr_F$ (100 μL, 4 μmol). In one case (R^0_{BTAIle} = 1.22), dimethyl itaconate (400 μmol) was also added to the catalytic mixtures. The resulting solutions were left to evaporate overnight in a fume hood. The resulting solids were put under vacuum (10^{-3} mbar) for 3 h before the addition of 1.0 mL of cyclohexane. The Eppendorf

DOI: 10.1021/jacs.6b01306
J. Am. Chem. Soc. 2016, 138, 4908−4916

tubes were sonicated for 1 min before centrifugation using a Gilson GmCLab at 6000 rpm for 30 min. The resulting solids and supernatants were then separated. The solids were dried under vacuum (10^{-3} mbar) for 3 h.

FT-IR Measurements. FT-IR measurements were performed on a Nicolet iS10 spectrometer. Solution spectra were measured in KBr or CaF_2 cells of 0.5 or 1.0 mm path length and were corrected for air, solvent, and cell absorption. FT-IR spectra of the solids were recorded after evaporation of a $CHCl_3$ solution (8.85 g L^{-1}) of the sample over KBr pellets.

Circular Dichroism (CD). CD measurements were performed on a Jasco J-1500 spectrometer equipped with a Peltier thermostated cell holder and Xe laser (lamp XBO 150W/4). Data were recorded at 20 °C with the following parameters: 20 nm min^{-1} sweep rate, 0.05 nm data pitch, 1.0 nm bandwidth, and between 350 and 180 nm. The obtained signals were processed as follows: solvent and cell contribution was subtracted, and the signals were smoothed (Savitzky−Golay method). Spectra were corrected for solvent and cell contribution. Kuhn anisotropy factors (g) are dimensionless and expressed as follows: $g = \theta/(32\,980 \times \mathrm{Abs})$, where θ is the measured ellipticity (mdeg) and Abs is the absorbance measured at the same wavelength. For CD measurements in solution, a 1 mm quartz cell (cyclohexane phase of catalytic mixtures) or a 0.1 mm dismountable quartz cell (mixtures of **BTA^{PPh2}** and **BTA Ile**) was used. Molar CD values are reported in L mol^{-1} cm^{-1} and are expressed as follows: $\Delta\varepsilon = \theta/(32\,980 \times l \times c)$ where θ is the measured ellipticity (mdeg), l is the optical path length in cm, and c is the total concentration ([**BTA^{PPh2}**] + [**BTA Ile**]) in mol L^{-1}. For all samples, LD contribution was negligible (ΔLD < 0.005 dOD). For CD measurements of solids, a $CHCl_3$ solution (8.85 g L^{-1}) of the sample was spin coated over a quartz plate using a Laurell WS-650-23 spin coater (3000 rpm). For all of the samples, no linear dichroism effects were present, and the shape of the CD signal was independent of the orientation of the quartz slide.

UV Spectroscopy. UV absorption spectra were extracted from CD analyses on each of the above samples and obtained after correction for air, solvent, and cell absorption.

Small-Angle Neutron Scattering (SANS) Analyses. SANS measurements were made at the LLB (Saclay, France) on the Pace instrument, at two distance−wavelength combinations to cover the 4 × 10^{-3} to 0.24 $Å^{-1}$ q-range, where the scattering vector q is defined as usual, assuming elastic scattering, as $q = (4\pi/\lambda)\sin(\theta/2)$, where θ is the angle between incident and scattered beam. Data were corrected for the empty cell signal and the solute and solvent incoherent background. A light water standard was used to normalize the scattered intensities to cm^{-1} units.

■ ASSOCIATED CONTENT

Supporting Information

The Supporting Information is available free of charge on the ACS Publications website at DOI: 10.1021/jacs.6b01306.

Experimental procedures, including synthesis and characterization of BTAs and their precursors, additional catalytic experiments (Tables S1 and S2), and spectroscopic and scattering analyses (Figures S1−S9; Tables S3−S5) (PDF)

■ AUTHOR INFORMATION

Corresponding Author

*matthieu.raynal@upmc.fr

Notes

The authors declare no competing financial interest.

■ ACKNOWLEDGMENTS

This work was supported by the French Agence Nationale de la Recherche (project ANR-13-BS07-0021 SupraCatal). A.V.-F. would like to thank MINECO (CTQ2014-60256-P) for financial support. Jacques Jestin (LLB, Saclay) is acknowledged for assistance with SANS experiment, Nicolas Vanthuyne (iSm2, Marseille) for chiral HPLC analyses, Fabrice Mathevet (UPMC, Paris) for his help in the preparation of spin-coated samples, Bruno Giordano Alvarenga (UPMC, Paris) and Ludovic Dubreucq (UPMC, Paris) for their help in the synthesis and characterization of some precursors and BTA monomers, and Marta Serrano Torne (ICIQ, Tarragona) for her help in the preparation of the catalytic experiments.

■ REFERENCES

(1) (a) Siegel, J. S. *Chirality* **1998**, *10*, 24−27. (b) Bailey, J. *Origins Life Evol. Biospheres* **2001**, *31*, 167−183. (c) Cintas, P.; Viedma, C. *Chirality* **2012**, *24*, 894−908. (d) Hein, J. E.; Blackmond, D. G. *Acc. Chem. Res.* **2012**, *45*, 2045−2054.

(2) (a) Noyori, R.; Kitamura, M. *Angew. Chem., Int. Ed. Engl.* **1991**, *30*, 49−69. (b) Soai, K.; Shibata, T.; Morioka, H.; Choji, K. *Nature* **1995**, *378*, 767−768. (c) Feringa, B. L.; van Delden, R. A. *Angew. Chem., Int. Ed.* **1999**, *38*, 3419−3438. (d) Todd, M. H. *Chem. Soc. Rev.* **2002**, *31*, 211−222. (e) Klussmann, M.; Iwamura, H.; Mathew, S. P.; Wells, D. H.; Pandya, U.; Armstrong, A.; Blackmond, D. G. *Nature* **2006**, *441*, 621−623. (f) Noorduin, W. L.; Izumi, T.; Millemaggi, A.; Leeman, M.; Meekes, H.; Van Enckevort, W. J. P.; Kellogg, R. M.; Kaptein, B.; Vlieg, E.; Blackmond, D. G. *J. Am. Chem. Soc.* **2008**, *130*, 1158−1159. (g) Satyanarayana, T.; Abraham, S.; Kagan, H. B. *Angew. Chem., Int. Ed.* **2009**, *48*, 456−494. (h) Soai, K.; Kawasaki, T.; Matsumoto, A. *Acc. Chem. Res.* **2014**, *47*, 3643−3654. (i) Dijken, D. J.; Beierle, J. M.; Stuart, M. C. A.; Szymanski, W.; Browne, W. R.; Feringa, B. L. *Angew. Chem., Int. Ed.* **2014**, *53*, 5073−5077. (j) Kawasaki, T.; Araki, Y.; Hatase, K.; Suzuki, K.; Matsumoto, A.; Yokoi, T.; Kubota, Y.; Tatsumi, T.; Soai, K. *Chem. Commun.* **2015**, *51*, 8742−8744. (k) Bukhryakov, K. V.; Almahdali, S.; Rodionov, V. O. *Langmuir* **2015**, *31*, 2931−2935.

(3) (a) Yashima, E.; Matsushima, T.; Okamoto, Y. *J. Am. Chem. Soc.* **1995**, *117*, 11596−11597. (b) Yashima, E.; Matsushima, T.; Okamoto, Y. *J. Am. Chem. Soc.* **1997**, *119*, 6345−6359.

(4) (a) Aparicio, F.; Matesanz, E.; Sanchez, L. *Chem. Commun.* **2012**, *48*, 5757−5759. (b) Duan, P. F.; Cao, H.; Zhang, L.; Liu, M. H. *Soft Matter* **2014**, *10*, 5428−5448.

(5) Eelkema, R.; Feringa, B. L. *Org. Biomol. Chem.* **2006**, *4*, 3729−3745.

(6) Shimomura, K.; Ikai, T.; Kanoh, S.; Yashima, E.; Maeda, K. *Nat. Chem.* **2014**, *6*, 429−434.

(7) (a) Yamamoto, T.; Adachi, T.; Suginome, M. *ACS Macro Lett.* **2013**, *2*, 790−793. (b) Ke, Y.-Z.; Nagata, Y.; Yamada, T.; Suginome, M. *Angew. Chem., Int. Ed.* **2015**, *54*, 9333−9337. (c) Nagata, Y.; Nishikawa, T.; Suginome, M. *J. Am. Chem. Soc.* **2015**, *137*, 4070−4073.

(8) (a) Rowan, A. E.; Nolte, R. J. M. *Angew. Chem., Int. Ed.* **1998**, *37*, 63−68. (b) Pijper, D.; Feringa, B. L. *Soft Matter* **2008**, *4*, 1349−1372.

(9) (a) Green, M. M.; Park, J. W.; Sato, T.; Teramoto, A.; Lifson, S.; Selinger, R. L. B.; Selinger, J. V. *Angew. Chem., Int. Ed.* **1999**, *38*, 3139−3154. (b) Maeda, K.; Yashima, E. *Top. Curr. Chem.* **2006**, *265*, 47−88. (c) Yashima, E.; Maeda, K.; Iida, H.; Furusho, Y.; Nagai, K. *Chem. Rev.* **2009**, *109*, 6102−6211.

(10) (a) Palmans, A. R. A.; Meijer, E. W. *Angew. Chem., Int. Ed.* **2007**, *46*, 8948−8968. (b) Liu, M. H.; Zhang, L.; Wang, T. Y. *Chem. Rev.* **2015**, *115*, 7304−7397.

(11) Lockman, J. W.; Paul, N. M.; Parquette, J. R. *Prog. Polym. Sci.* **2005**, *30*, 423−452.

(12) (a) Green, M. M.; Reidy, M. P.; Johnson, R. J.; Darling, G.; Oleary, D. J.; Willson, G. *J. Am. Chem. Soc.* **1989**, *111*, 6452−6454. (b) Green, M. M.; Garetz, B. A.; Munoz, B.; Chang, H. P.; Hoke, S.; Cooks, R. G. *J. Am. Chem. Soc.* **1995**, *117*, 4181−4182.

(13) (a) Green, M. M.; Peterson, N. C.; Sato, T.; Teramoto, A.; Cook, R.; Lifson, S. *Science* **1995**, *268*, 1860−1866. (b) van Gestel, J.; van der Schoot, P.; Michels, M. A. J. *Macromolecules* **2003**, *36*, 6668−6673. (c) van Gestel, J. *Macromolecules* **2004**, *37*, 3894−3898. (d) van

DOI: 10.1021/jacs.6b01306
J. Am. Chem. Soc. 2016, 138, 4908−4916

Gestel, J.; van der Schoot, P.; Michels, M. A. J. *J. Chem. Phys.* **2004**, *120*, 8253−8261. (e) Markvoort, A. J.; ten Eikelder, H. M. M.; Hilbers, P. A. J.; de Greef, T. F. A.; Meijer, E. W. *Nat. Commun.* **2011**, *2*, 509−517. (f) ten Eikelder, H. M. M.; Markvoort, A. J.; de Greef, T. F. A.; Hilbers, P. A. J. *J. Phys. Chem. B* **2012**, *116*, 5291−5301. (g) Jabbari-Farouji, S.; van der Schoot, P. *J. Chem. Phys.* **2012**, *137*, 064906.

(14) For a review on asymmetric catalysis with helical polymers, see: Megens, R. P.; Roelfes, G. *Chem. - Eur. J.* **2011**, *17*, 8514−8523.

(15) The presence of a large amount of phosphine-free monomers, used in combination with the phosphine monomers and the chiral comonomers, is a characteristic of this class of helical catalysts because phosphine-rich polymers were found to be less selective: Yamamoto, T.; Suginome, M. *Angew. Chem., Int. Ed.* **2009**, *48*, 539−542.

(16) Poly(phenylacetylene) copolymers composed of achiral imidazolidinone monomers and chiral comonomers were also investigated but provided modest enantioselectivity in Diels−Alder reactions: Takata, L. M. S.; Iida, H.; Shimomura, K.; Hayashi, K.; dos Santos, A. A.; Yashima, E. *Macromol. Rapid Commun.* **2015**, *36*, 2047−2054.

(17) (a) Huerta, E.; van Genabeek, B.; Lamers, B. A. G.; Koenigs, M. M. E.; Meijer, E. W.; Palmans, A. R. A. *Chem. - Eur. J.* **2015**, *21*, 3682−3690. (b) Neumann, L. N.; Baker, M. B.; Leenders, C. M. A.; Voets, I. K.; Lafleur, R. P. M.; Palmans, A. R. A.; Meijer, E. W. *Org. Biomol. Chem.* **2015**, *13*, 7711−7719.

(18) de Torres, M.; van Hameren, R.; Nolte, R. J. M.; Rowan, A. E.; Elemans, J. A. A. W. *Chem. Commun.* **2013**, *49*, 10787−10789.

(19) Raynal, M.; Portier, F.; van Leeuwen, P. W. N. M.; Bouteiller, L. *J. Am. Chem. Soc.* **2013**, *135*, 17687−17690.

(20) (a) Tam, A. Y. Y.; Wong, K. M. C.; Yam, V. W. W. *Chem. - Eur. J.* **2009**, *15*, 4775−4778. (b) Po, C.; Ke, Z. H.; Tam, A. Y. Y.; Chow, H. F.; Yam, V. W. W. *Chem. - Eur. J.* **2013**, *19*, 15735−15744. (c) Zhu, L. L.; Li, X.; Wu, S. J.; Nguyen, K. T.; Yan, H.; Agren, H.; Zhao, Y. L. *J. Am. Chem. Soc.* **2013**, *135*, 9174−9180. (d) Jung, S. H.; Jeon, J.; Kim, H.; Jaworski, J.; Jung, J. H. *J. Am. Chem. Soc.* **2014**, *136*, 6446−6452. (e) Dubarle-Offner, J.; Moussa, J.; Amouri, H.; Jouvelet, B.; Bouteiller, L.; Raynal, M. *Chem. - Eur. J.* **2016**, *22*, 3985−3990.

(21) Jin, Q. X.; Zhang, L.; Cao, H.; Wang, T. Y.; Zhu, X. F.; Jiang, J.; Liu, M. H. *Langmuir* **2011**, *27*, 13847−13853.

(22) For leading examples of asymmetric catalysis performed with a combination of an achiral or racemic metal complex and a chiral inducer, see: (a) Faller, J. W.; Lavoie, A. R.; Parr, J. *Chem. Rev.* **2003**, *103*, 3345−3367. (b) Mikami, K.; Yamanaka, M. *Chem. Rev.* **2003**, *103*, 3369−3400. (c) Hamilton, G. L.; Kang, E. J.; Mba, M.; Toste, F. D. *Science* **2007**, *317*, 496−499. (d) Ding, K. L. *Chem. Commun.* **2008**, 909−921. (e) Nishioka, Y.; Yamaguchi, T.; Kawano, M.; Fujita, M. *J. Am. Chem. Soc.* **2008**, *130*, 8160−8161. (f) Boersma, A. J.; Megens, R. P.; Feringa, B. L.; Roelfes, G. *Chem. Soc. Rev.* **2010**, *39*, 2083−2092. (g) Park, S.; Sugiyama, H. *Angew. Chem., Int. Ed.* **2010**, *49*, 3870−3878. (h) Ward, T. R. *Acc. Chem. Res.* **2011**, *44*, 47−57. (i) Lo, C.; Ringenberg, M. R.; Gnandt, D.; Wilson, Y.; Ward, T. R. *Chem. Commun.* **2011**, *47*, 12065−12067. (j) Dydio, P.; Rubay, C.; Gadzikwa, T.; Lutz, M.; Reek, J. N. H. *J. Am. Chem. Soc.* **2011**, *133*, 17176−17179. (k) van Leeuwen, P. W. N. M.; Rivillo, D.; Raynal, M.; Freixa, Z. *J. Am. Chem. Soc.* **2011**, *133*, 18562−18565. (l) Mahlau, M.; List, B. *Isr. J. Chem.* **2012**, *52*, 630−638. (m) Phipps, R. J.; Hamilton, G. L.; Toste, F. D. *Nat. Chem.* **2012**, *4*, 603−614. (n) Ohmatsu, K.; Ito, M.; Kunieda, T.; Ooi, T. *Nat. Chem.* **2012**, *4*, 473−477. (o) Ohmatsu, K.; Ito, M.; Kunieda, T.; Ooi, T. *J. Am. Chem. Soc.* **2013**, *135*, 590−593. (p) Wang, L. X.; Xiang, J. F.; Tang, Y. L. *Adv. Synth. Catal.* **2015**, *357*, 13−20.

(23) For the chirality amplification properties of alkyl BTAs, see: (a) Smulders, M. M. J.; Schenning, A. P. H. J.; Meijer, E. W. *J. Am. Chem. Soc.* **2008**, *130*, 606−611. (b) Smulders, M. M. J.; Filot, I. A. W.; Leenders, J. M. A.; Van der Schoot, P.; Palmans, A. R. A.; Schenning, A. P. H. J.; Meijer, E. W. *J. Am. Chem. Soc.* **2010**, *132*, 611−619. (c) Smulders, M. M. J.; Stals, P. J. M.; Mes, T.; Pfaffen, T. F. E.; Schenning, A. P. H. J.; Palmans, A. R. A.; Meijer, E. W. *J. Am. Chem. Soc.* **2010**, *132*, 620−626. (d) Stals, P. J. M.; Smulders, M. M. J.; Martín-Rapún, R.; Palmans, A. R. A.; Meijer, E. W. *Chem. - Eur. J.* **2009**, *15*, 2071−2080.

(24) (a) de Loos, M.; van Esch, J. H.; Kellogg, R. M.; Feringa, B. L. *Tetrahedron* **2007**, *63*, 7285−7301. (b) Veld, M. A. J.; Haveman, D.; Palmans, A. R. A.; Meijer, E. W. *Soft Matter* **2011**, *7*, 524−531. (c) Desmarchelier, A.; Raynal, M.; Brocorens, P.; Vanthuyne, N.; Bouteiller, L. *Chem. Commun.* **2015**, *51*, 7397−7400.

(25) Fernandez-Perez, H.; Donald, S. M. A.; Munslow, I. J.; Benet-Buchholz, J.; Maseras, F.; Vidal-Ferran, A. *Chem. - Eur. J.* **2010**, *16*, 6495−6508.

(26) In contrast to this observation, the conformation of poly(quinoxaline-2,3-diyl)s polymers is strongly affected by the nature of the alkane solvent. It led to inversion of the major enantiomer obtained, for example, in *n*-octane and cyclooctane when these polymers were used as scaffolds for catalysis. See: Nagata, Y.; Nishikawa, T.; Suginome, M. *J. Am. Chem. Soc.* **2014**, *136*, 15901−15904.

(27) The effect of the amount of chiral comonomer on the selectivity displayed by **BTA Val** was not probed. However, catalytic experiments performed with different amounts of **BTA Nle** and a fixed amount of **BTA^{PPh2}** showed the same trend as that observed for **BTA Ile**: 55% ee (R^0_{BTANle} = 0.25), 74% ee (R^0_{BTANle} = 1.25), and 35% ee (R^0_{BTANle} = 4.0)

(28) Suginome and co-workers reported a decrease of the enantioselectivity for the palladium-catalyzed hydrosilylation of styrene in presence of poly(quinoxaline-2,3-diyl)s ligands incorporating more than 15% chiral units. It was attributed to higher disorder of the helical structure as a result of steric repulsion imposed by the bulky chiral groups. See ref 7a.

(29) Cyclohexane has been used for spectroscopic characterizations, instead of hexane/CH_2Cl_2 (10:1) in the case of catalytic experiments.

(30) According to the assignment made by Meijer and co-workers: Nakano, Y.; Hirose, T.; Stals, P. J. M.; Meijer, E. W.; Palmans, A. R. A. *Chem. Sci.* **2012**, *3*, 148−151.

(31) Jana, P.; Paikar, A.; Bera, S.; Maity, S. K.; Haldar, D. *Org. Lett.* **2014**, *16*, 38−41.

(32) Roosma, J.; Mes, T.; Leclère, P.; Palmans, A. R. A.; Meijer, E. W. *J. Am. Chem. Soc.* **2008**, *130*, 1120−1121.

(33) For all of the solids, no linear dichroism effects were present, and the shape of the CD signal was independent of the orientation of the quartz slide.

(34) In these structures, we arbitrarily chose that the three amide groups are oriented in the same direction despite the fact that an "asymmetric" orientation of the amide groups is also plausible, see: Bejagam, K. K.; Fiorin, G.; Klein, M. L.; Balasubramanian, S. *J. Phys. Chem. B* **2014**, *118*, 5218−5228.

(35) The relative *Re* or *Si* configuration of the *meta*-substituted aryl *Z* rings is not known. Chirality transfer from stacked aromatic rings to prochiral metals is known for disubstituted ferrocene peptides[35a] and has been postulated for supramolecular catalysts.[22k,35b−f] For one example of chirality transfer in covalent asymmetric catalysts, see ref 35g. (a) Kirin, S. I.; Kraatz, H. B.; Metzler-Nolte, N. *Chem. Soc. Rev.* **2006**, *35*, 348−354. (b) Laungani, A. C.; Breit, B. *Chem. Commun.* **2008**, 844−846. (c) Laungani, A. C.; Slattery, J. M.; Krossing, I.; Breit, B. *Chem. - Eur. J.* **2008**, *14*, 4488−4502. (d) Kokan, Z.; Kirin, S. I. *RSC Adv.* **2012**, *2*, 5729−5737. (e) Kokan, Z.; Kirin, S. I. *Eur. J. Org. Chem.* **2013**, *2013*, 8154−8161. (f) Kokan, Z.; Glasovac, Z.; Elenkov, M. M.; Gredicak, M.; Jeric, I.; Kirin, S. I. *Organometallics* **2014**, *33*, 4005−4015. (g) Yu, J. F.; RajanBabu, T. V.; Parquette, J. R. *J. Am. Chem. Soc.* **2008**, *130*, 7845−7847.

(36) Bissette, A. J.; Fletcher, S. P. *Angew. Chem., Int. Ed.* **2013**, *52*, 12800−12826.

(37) Neumann, E.; Pfaltz, A. *Organometallics* **2005**, *24*, 2008−2011.

DOI: 10.1021/jacs.6b01306
J. Am. Chem. Soc. 2016, 138, 4908−4916